Selective serotonin reuptake inhibitors directly signal for apoptosis in biopsy-like Burkitt lymphoma cells

Adamantios Serafeim, Michelle J. Holder, Gillian Grafton, Anita Chamba, Mark T. Drayson, Quang T. Luong, Christopher M. Bunce, Christopher D. Gregory, Nicholas M. Barnes, and John Gordon

Selective serotonin reuptake inhibitors (SSRIs) are the treatment of choice for clinical depression and a range of anxiety-related disorders. They are well tolerated over extended periods with more than 50 million people worldwide benefiting from their use. Here we show that 3 structurally distinct SSRIs—fluoxetine, paroxetine, and citalopram—act directly on Burkitt lymphoma (BL) cells to trigger rapid and extensive programmed cell death. SSRIs unexpectedly stimulated calcium flux, tyrosine phosphorylation, and down-regulation of the c-*myc* and *nm23* genes in Burkitt lymphoma cells remaining faithful to the biopsy phenotype. Resultant SSRI-induced apoptosis was preceded by caspase activation, poly(ADP-ribose) polymerase-1 (PARP-1) cleavage, DNA fragmentation, a loss of mitochondrial membrane potential, and the externalization of phosphatidylserine, and reversed by the overexpression of *bcl*-2. Normal peripheral blood mononuclear cells and tonsil B cells, whether resting or stimulated into cycle, were largely resistant to SSRI-induced death as were 5 non-BL lymphoid cell lines tested. We discuss these findings within the context of whether the SSRI class of antidepressants could find future application as potential therapeutics for the highly aggressive and—because of its association with AIDS—increasingly more common Burkitt lymphoma. (Blood. 2003;101: 3212-3219)

© 2003 by The American Society of Hematology

Introduction

Burkitt lymphoma (BL) is a highly malignant tumor characterized uniquely by a 100% mitotic index among the constituent cells.[1] The tumor—which tends to develop extra-nodally, with a preference for the jaw and abdomen—can double in size within a day and remains a serious health problem in those areas where it is endemic: namely, the malarial belts of equatorial Africa, northeastern Brazil, and Papua New Guinea.[2] The often limited medical resources in these regions can compromise the survival rates that can be achieved with current protocols of aggressive combination chemotherapy continued over several months and requiring frequent hospitalizations.[3] Outside of endemic regions, the incidence of Burkitt lymphoma has increased dramatically in the past 2 decades because of its association with HIV infection, such that within North America, for example, there is a 1000-fold increased incidence among individuals with AIDS.[4,5] The median survival of HIV-positive patients with non-Hodgkin lymphomas, of which BL comprises some 20%, is only 6 months.[6] Even among HIV-negative individuals in which there is a 3-year relapse-free survival rate of approximately 80% for BL patients with local disease, those with disseminated tumor respond poorly to chemotherapy and have lower survival rates.[3]

Regardless of geographic origin or HIV association, BL is characterized by translocations of one c-*myc* allele to one of the immunoglobulin loci, and the extraordinarily high growth rate that characterizes these tumors reflects the proproliferative actions of the translocated gene.[7-9] However, despite translocation to immunoglobulin loci, the BL-associated constitutive expression of c-*myc* remains dependent on the binding of the recognized c-*myc* transcription factor Nm23-H2 to a PuF site within the regulatory sequence of the translocated gene.[10] A recent report has identified that expression of Nm23-H1 may also be linked to c-*myc* expression, and the high expression of the gene has been correlated with poor responses to treatment in high-grade lymphoma in general.[11-12] Deregulated c-*myc* expression likely contributes to what appears an apparent dichotomy in the pathobiology of BL: namely aggressive, uncontrolled proliferation coupled with high-rate apoptosis. The latter attribute gives rise to the classical "starry sky" histology that characterizes BL, reflecting the presence of large tingible body macrophages that have been mobilized to the tumor in order to clear the large burden of apoptotic cells generated at these sites.[1,13,14] Reflecting their normal physiologic counterpart—the B cell proliferating in the germinal centers of secondary lymphoid tissues—BL cells in situ are negative for, or only weakly express, the antiapoptotic survival gene *bcl*-2.[14-17] This feature is retained in BL lines held in early passage. Indeed, "biopsy-like" (so-called "group I") BL cell lines stay remarkably faithful to the in

---

situ phenotype, and thereby provide excellent models for examining treatments that might serve to shift the damaging imbalance between proliferation and apoptosis in the tumor in such a way as to favor the latter.[18-19]

We have recently reported on the serotonin transporter (SERT) as an unexpected candidate target for therapeutic attack in Burkitt lymphoma.[20] BL cells were shown to carry immunoreactive SERT and to transport 5-HT (serotonin) with appropriate first-order kinetics. Moreover, a capacity for 5-HT to drive rapid and extensive apoptosis in biopsy-like BL cells was largely reversed by the class of antidepressants known as the selective serotonin reuptake inhibitors (SSRIs) that act by blocking the active uptake of 5-HT into SERT-carrying cells.[20] We now report the surprising finding that the SSRIs themselves are capable of provoking apoptotic death in biopsy-like BL cell lines.

Materials and methods

Cells and cell lines

Early passage group I BL lines L3055 (EBV$^-$), Namalwa (EBV$^-$), BL2 (EBV$^-$), Elijah (EBV$^-$), and Mutu I (EBV$^+$), the late passage group III BL line Mutu III (EBV$^+$), NALM6 ("pre-B"), RPMI 8226 ("plasmacytoid"), and 3 T-cell lines—Jurkat, J10, and CEM—were maintained in RPMI 1640 medium supplemented with 10% Serum Supreme (BioWhittaker, Wokingham, United Kingdom), 2 mM glutamine, 100 IU/mL penicillin, and 100 μg/mL streptomycin as previously described.[21] Stable *bcl*-2 transfectants of L3055 cells, together with those carrying the mammalian expression vector pEF-MC1 neopA alone as controls, were as detailed elsewhere.[22] Resting B cells were isolated by negative depletion of tonsilar mononuclear cells using a magnetic cell separator to remove those bearing CD3, CD14, or CD38 exactly as described previously.[23]

Reagents

Fluoxetine (Prozac), 5-HT, fura-2, thapsigargin, and Ca^{2+}-free (low) medium were purchased from Sigma (Dorset, United Kingdom). Paroxetine (Paxil) and citalopram (Celexa) are from Smith-Kline Beecham (Harlow, Essex, United Kingdom) and Lundbeck (Copenhagen, Denmark), respectively. Affinity-purified goat F(ab′)$_2$ antibody to human immunoglobulin M (IgM) was purchased from ICN (Aurora, OH). Soluble recombinant human CD40 ligand (CD40L) was kindly provided by R. J. Armitage (Immunex, Seattle, WA). *Staphylococcus aureus* Cowan 1 (SAC) and ionomycin were from CN Biosciences (Nottingham, United Kingdom). The JC-1 (5,5′,6,6′-tetrachlorol, 1′,3,3′-tetraethylbenzimidazolyl-carbocyanine iodide) cationic dye and syto 16 was purchased from Molecular Probes (Leiden, Holland). The 4G10 anti–phosphotyrosine antibody was from Upstate Biotechnology (Milton Keynes, United Kingdom). Murine antibody to Bcl-2 (clone 124) was from Dako (Ely, United Kingdom); poly(ADP-ribose) polymerase-1 (PARP-1) antibody (clone A6.4.12) was from Insight Biotechnology (Wembley, United Kingdom). The supersignal chemiluminescence reagent and horseradish peroxidase (HRP)–conjugated rabbit antimouse antibody were from Pierce (Chester, United Kingdom). All other chemicals were obtained from Sigma (Poole, United Kingdom) and were of the best grade available. Where reagents were added to cell culture, the appropriate vehicle to the same dilution was used as control.

Assessment of DNA synthesis and cell-cycle status

DNA synthesis was determined by measuring ^{3}[H]-thymidine (^{3}[H]Tdr; Amersham, Little Chalfont, United Kingdom) incorporation into cellular DNA as documented elsewhere.[21] Cell-cycle analysis of propidium iodide (PI)–stained cells was performed exactly as described previously with results expressed as percentage of viable cells residing in each phase of the cycle.[24]

Viability assays

Changes in the viability of cells cultured under conditions indicated were quantified by assessment of forward and 90° (side) light scatter of cells using an EPICS XL-MCL flow cytometer (Beckman Coulter, Miami, FL) with cells gated into 2 populations (viable and dead) as described elsewhere.[20] Cells were also analyzed in order to assess the percentages within treated populations of those that were viable, apoptotic, or necrotic, as described in Milner et al.[25] Analysis by fluorescence-activated cell-sorter (FACS) generates a 2-dimensional plot of syto 16 fluorescence versus PI fluorescence: syto 16 is taken up by only viable cells, whereas PI exclusively enters necrotic cells—syto 16$^-$/PI$^-$ cells are deemed apoptotic.[20,25]

Measures of apoptosis

Apoptosis was assessed by staining cells with acridine orange and visualizing nuclear morphology exactly as described previously.[24] Viable cells display a homogeneous chromatin-staining pattern, whereas apoptotic cells characteristically show condensed and fragmented chromatin. Mitochondrial depolarization was assessed using the JC-1 cationic dye.[20] JC-1 exhibits potential-dependent accumulation in mitochondria accompanied by a shift in fluorescence emission from 525 nm (green) to 590 nm (red). Mitochondrial depolarization is indicated by a decrease in the red-green fluorescence ratio as described previously.[20] Caspase activity was detected using the CaspaTag Caspace Activity Kit (Intergen, Oxford, United Kingdom). Cells cultured under the conditions indicated in the text were stained using FAM-VAD-FMK together with PI (to distinguish dead cells from live cells) then analyzed on an EPICS XL-MCL flow cytometer or by confocal microscopy (with the addition of Hoechst 33342 stain) exactly as described previously.[20] Phosphatidylserine exposure was measured using the Annexin V FITC Apoptosis Detection Kit from CN Biosciences, while TUNEL (terminal deoxynucleotidyl transferase [TdT]–mediated dUTP-biotin nick end-labeling) was performed using the ApopTag Fluorescein Direct In situ Apoptosis Detection Kit from Flowgen (Ashby de la Zouch, United Kingdom), both in accord with the manufacturer's instructions.

Calcium measurements

Cells (5×10^7/mL) were resuspended in culture medium, and loaded with 1 μM of fura-2 for 45 minutes at 37°C. At the end of the incubation they were washed twice with Hanks buffered saline solution (HBSS) containing 10% fetal calf serum (FCS) and 10 mM HEPES (*N*-2-hydroxyethylpiperazine-*N*′-2-ethanesulfonic acid, pH 7.2), resuspended at 4×10^6/mL, and stored on ice until used. Measurements were performed using a Hitachi F2500 fluorescence spectrophotometer (Tokyo, Japan), with excitation wavelengths of 340 nm and 380 nm and emission wavelengths of 510 nm. Cells were incubated at 37°C for 5 minutes prior to use. Maximum response was obtained following addition of 0.05% TX100 plus 0.01 mM DETAPAC (diethylenetriaminepentaacetic acid); minimum values were obtained following addition of 10 mM EGTA (ethylene glycol tetraacetic acid) plus 30 mM Tris (tris(hydroxymethyl)aminomethane, pH 7.2). In preliminary experiments it was established that there was no significant dye leakage for at least 2 hours after loading of the cells, and that the SSRIs did not exhibit significant autofluorescence.

Western blots

For assessment of tyrosine phsophorylation, cells were lysed in radioimmunoprecipitation assay (RIPA) buffer, separated on sodium dodecyl sulfate–polyacrylamide gel electrophoresis (SDS-PAGE), transferred to polyvinylidene fluoride (PVDF) membranes, and probed with the 4G10 anti–phosphotyrosine antibody. Protein (25 μg) was loaded onto each lane. Blots were developed with an HRP-conjugated antimouse secondary antibody and visualized using an enhanced chemiluminescence method.[20] Bcl-2 and PARP-1 blots were performed exactly as described elsewhere.[21,26]

Real-time PCR quantification of gene expression

Reactions were performed using an ABI Prism 7700 sequence detector (Applied Biosystems, Foster City, CA) with 18S ribosomal RNA as the

internal standard. Gene-specific primers were synthesized by Alta Bio-science (University of Birmingham) and probes by Applied Biosystems. Each reaction contained 900 nM of gene-specific 5′ and 3′ primers; 1X Mastermix (containing preoptimized deoxynucleoside triphosphate [dNTP], MgCl₂, and buffer concentrations; Applied Biosystems); 125 to 175 nM gene-specific probe (5′-6-FAM, 3′-TAMRA labeled); 50 nM 18S 5′ and 3′ primers, and 200 nM 18S probe (5′-VIC, 3′-TAMRA labeled); and 0.25 μL cDNA (equivalent to 12.5 ng reverse-transcribed RNA), in a total volume of 25 μL. Reactions were replicated 3 times on a 96-well plate format. nm23-H1 reactions used 5′ primer 5′-GGCCTGGTGAAATACATGCA-3′, 3′ primer 5′-GGCCCGTCTTCACCACAT-3′, and probe 5′-6-FAM-CTCCCAGACCATGGCAACTACCGG-TAMRA-3′. nm23-H2 reactions used 5′ primer 5′-CTGGTGGGCGAGATCATCA-3′, 3′ primer 5′-TGTAGTGCTGCTTCAGGTGTTCTT-3′, and probe 5′-6-FAM-CCAT-GAAGTTCCTCCGGGCCTCTG-TAMRA-3′. c-myc reactions used 5′ primer TCAAGAGGTGCCACGTCTCC-3′, 3′ primer 5′-TCTTGGCAG-CAGGATAGTCCTT-3′, and probe 5′-6-FAM-CAGCACAACTACG-CAGCGCCTCC-TAMRA-3′. Regulation of c-myc, nm23-H1, and nm23-H2 was compared with that of the housekeeping gene cyclophilin A. For these assays, commercially available primers and probes were used as described by the manufacturer's instructions (Applied Biosystems catalog no. 4310883E). Cycle threshold (Ct) values were obtained graphically for test genes and 18S internal standard. Gene expression was normalized to the 18S and represented as ΔCt values. Comparison of gene expression between control and treated samples was derived from subtraction of control ΔCt values from treatment ΔCt values to give a ΔΔCt value and relative gene expression was calculated as $2^{-\Delta\Delta Ct}$ and normalized to controls. Where statistical comparisons have been made we have used ΔCt values and paired t tests.

Results

SSRIs inhibit DNA synthesis in biopsy-like BL cells

BL cells kept in early passage closely resemble those of the original biopsy. This includes a tendency for background (spontaneous) apoptosis coupled to a remarkably high rate of proliferation.[18,19,27] Results illustrated in Figure 1A-C demonstrate that the chemically distinct SSRIs (fluoxetine, paroxetine, and citalopram) each inhib-ited—in a concentration-dependent fashion—DNA synthesis occur-ring in the prototypic BL cell line, L3055. The potencies of the SSRIs in this regard are lower than their EC_{50} (concentration

invoking half-maximal effect) for SERT blockade.[28] Nonetheless, similar inhibition was found in 5 of 5 distinct BL cell lines held in early passage (Figure 1D). This included the Mutu I cell line that on long-term in vitro propagation drifts to what is known as a "group III" phenotype due to the activation of endogenous Epstein-Barr virus (EBV)–transforming genes that are otherwise latent in the original biopsy and early passage cells.[18,19] As has been found for other antiproliferative signals,[20,24,27,29] progression to the group III status—as exemplified here by Mutu III—also renders BL cells refractory to the inhibitory actions of the SSRIs (Figure 1D).

SSRI-inhibited DNA synthesis within biopsy-like BL cultures was accompanied by an accumulation of cells at the G_0/G_1 stage of cell cycle similar to that previously described following cross-linking of the B-cell antigen receptor (BCR) and achieved here using antibody to μ heavy chain of surface IgM (Figure 1E).[24] Cell-cycle arrest in BL cells on BCR cross-linking is followed by entry into apoptosis: this can be reversed through CD40 on the BL cells engaging CD40 ligand (CD40L/CD154).[17,21,22,24] The results in Figure 1F show that while CD40L had a minimal effect on the cessation of DNA synthesis promoted by SSRIs (illustrated here by fluoxetine), it substantially reversed the cell death that was otherwise occurring on fluoxetine exposure (as judged by character-istic changes in light-scatter properties in otherwise homogenous viable BL populations[30]).

Characteristics of SSRI-promoted cell death in BL cells

To address the nature of BL cell death promoted by the SSRIs we turned to a number of approaches. Figure 2A shows that fluoxetine, in a concentration-dependent manner, drastically reduced the number of cells remaining viable at 24 hours as determined by a loss of cells capable of taking up the vital dye, syto 16 (green). This loss of viability was accompanied by an increasing number of cells becoming apoptotic (syto $16^-/PI^-$ [blue]) and/or necrotic (syto $16^-/PI^+$ [red]); such determination was based on the differential ability of PI to be excluded from or to enter cells undergoing apoptosis or necrosis, respectively. The appearance of cells in the "necrotic" gate in response to SSRI treatment likely reflects necrosis secondary to apoptosis (in the absence of cells that would otherwise elicit phagocytic clearance in an in vivo setting).
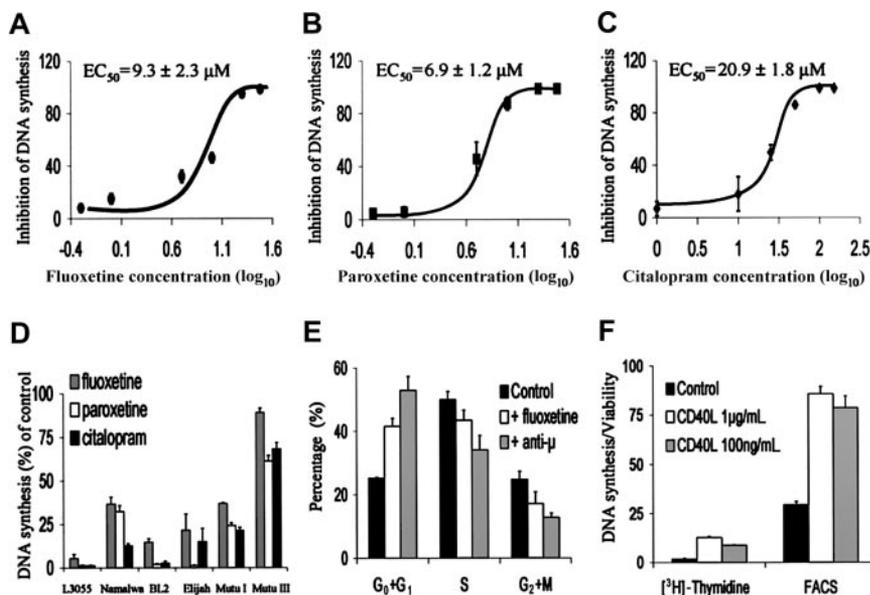

Figure 1. Fluoxetine promotes growth cessation in biopsy-like Burkitt lymphoma cells. L3055 cells were treated for 24 hours with (A) 0.5 to 30 μM fluoxetine; (B) 0.5 to 30 μM paroxetine; and (C) 1 to 150 μM citalopram; EC_{50} values of DNA synthesis inhibition for each of the SSRIs are indicated. (D) 5 group I BL lines and the group III cell line "Mutu III" were treated for 24 hours with fluoxetine (20 μM, ▨), paroxetine (20 μM, ☐), or citalo-pram (100 μM, ■), and resultant DNA synthesis ex-pressed as percent control. (E) L3055 cells cultured for 24 hours either alone (■), with fluoxetine (20 μM, ☐), or with anti-μ chain antibody (10 μg/mL, ▨), and viable population subjected to cell-cycle analysis. (F) L3055 cells pretreated for 1 hour with soluble CD40L trimer were then cultured for 24 hours before analysis of DNA synthesis (³[H]-thymidine) and cell viability (FACS); re-sults are percent change due to presence of 20 μM fluoxetine. All data are means ± SEMs, from 8 separate experiments for panel A; 6, for panels B-D; and 3, for panels E-F.
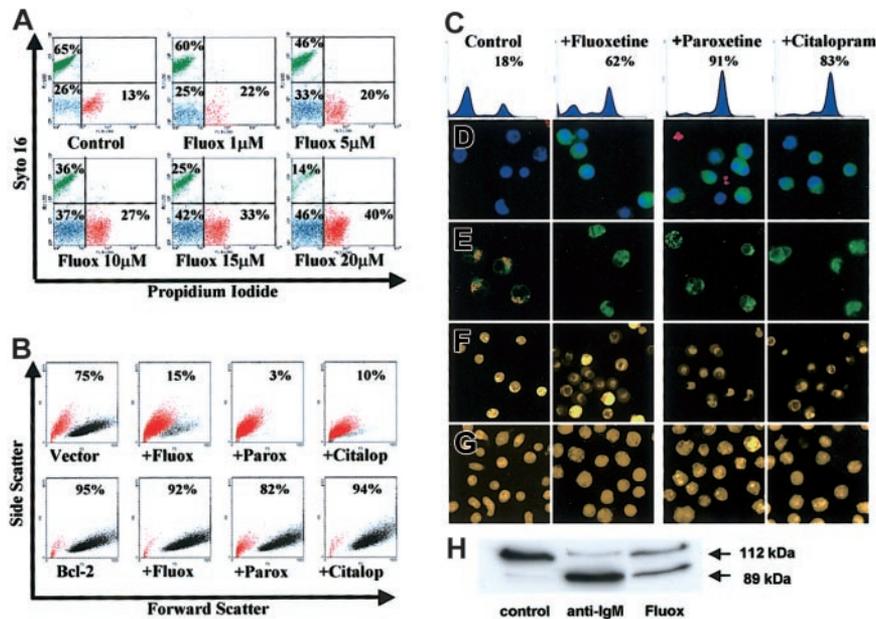
Figure 2. Characteristics of SSRI-induced apoptosis in group I BL cells. (A) L3055 cells treated with fluoxetine for 24 hours then double stained with syto 16 and PI for FACS analysis; percent cells viable (green), apoptotic (blue), and necrotic (red) are indicated. (B) L3055 transfected with either *bcl*-2, or empty vector treated for 24 hours with control medium, 20 μM fluoxetine, 20 μM paroxetine, or 100 μM citalopram, before analysis for forward versus side scatter. Percent viable cells remaining (black dots) are indicated; dead cells are in red. (C-E) L3055 cells were treated with SSRIs as for panel B. (C-D) Cells were treated for 6 hours and then stained for active caspases before analysis by (C) flow cytometry (percent cells active caspase positive indicated) or (D) confocal microscopy, counterstained with Hoechst nuclear dye (blue) and PI to detect dead and membrane-compromised cells (red) (activated caspases stain green). (E) Cells were treated for 24 hours, then stained with the cationic dye JC-1 for confocal microscopy. Mitochondrial depolarization is indicated by a shift from red to green fluorescence. (F) Cells were treated for 24 hours, then stained with the acridine orange for fluorescence microscopy. (G) Cells were treated as for panel F but using L3055 *bcl*-2-transfectants. (H) L3055 cells were cultured for 17 hours with either control medium, anti-μ chain antibody (anti-IgM, 10 μg/mL), or fluoxetine (20 μM); cell lysates prepared and equal amounts of protein (25 μg) resolved on 10% SDS-PAGE before blotting for PARP-1. The intact 112-kDa and cleaved 89-kDa protein are indicated by arrows. Each result is representative of at least 3 individual experiments.

Results from Figure 2B confirm the importance of the apoptotic pathway in the SSRI-induced cell death, as overexpression of antiapoptotic Bcl-2 protected the BL cells from all 3 drugs tested. Thus while cells carrying empty (control) vector lost the light-scatter characteristics of the viable subpopulation (indicated in black) and moved to the dead gate (indicated in red) in response to SSRIs, those expressing the vector containing *bcl*-2 remained in the viable sector.

Each of the SSRIs promoted caspase activation in the BL cells as assessed by the carboxyfluorescent probe FAM-VAD-FMK that binds irreversibly to caspases in their active configuration. Increased activation of caspases over background levels in L3055 group I BL cells following 6 hours of treatment with the SSRIs can be seen both by FACS-based analysis (Figure 2C) and by laser-scanning confocal microscopy where the treated cells—counterstained by the Hoechst nuclear dye (blue) and with PI to reveal dead cells (red)—exhibit green cytoplasmic staining for active caspases (Figure 2D).

Staining of SSRI-treated L3055 cells with the carbocyanine liquid crystal–forming probe JC-1 highlighted a loss of mitochondrial membrane potential accompanying the drug-induced apoptosis of group I BL cells. Thus, following exposure to each of the SSRIs, there is a complete disappearance of the intense red emission from JC-1 aggregates, which in control cells form within mitochondria maintaining their membrane potential integrity; instead, SSRI-treated cells develop a diffuse green emission that results from the disseminated distribution of relatively unconcentrated JC-1 monomers (Figure 2E). The classic apoptotic morphology of condensed and fragmented nuclei revealed by staining cells with acridine orange was also evident after SSRI exposure (Figure 2F). Again, this was reversed by Bcl-2 overexpression (Figure 2G).

Attempts to address whether the SSRI-promoted caspase activation as shown in Figure 2C-D was leading directly to the observed apoptosis using the pancaspase inhibitor Z-VAD-FMK were thwarted because of deleterious effects on these cells by the inhibitor itself (J.G., unpublished observation, October 2001). We therefore asked whether a major downstream substrate of the caspase pathway, PARP-1, undergoes cleavage in biopsy-like BL cells as a result of fluoxetine action. Figure 2H shows the degree of PARP-1 cleavage following exposure of L3055 cells to either anti-IgM or fluoxetine for 17 hours. Whereas intact 112-kDa PARP-1 was the almost exclusive form in control cells, anti-IgM treatment resulted in most PARP-1 being cleaved to the p89 fragment; 20μM fluoxetine similarly promoted extensive PARP-1 cleavage.

Annexin V binding to phosphatidylserine exposed on the outer leaflet of cells to signal for phagocytic engulfment is another commonly used measure of programmed death, although caution should be applied when using as a sole indicator for assessing apoptosis in B cells.[31,32] We found that while untreated L3055 cells displayed low-level Annexin V binding on approximately half the cells, most cells developed a higher level of binding following their culture with either anti-IgM or fluoxetine (Table 1).

Neither BL cells nor their normal germinal center B-cell equivalents tend to produce the extensive "DNA ladders" that can be seen as a result of DNA fragmentation when other cells (eg, thymocytes) undergo apoptosis.[33,34] Nevertheless, we asked whether fluoxetine might be inducing the type of DNA breaks associated with apoptosis by using a TUNEL-based method in which cells are first treated with DNA ligase before assessing the incorporation by TdT of a fluorescent-labeled nucleotide into DNA with strand breaks having blunt ends or single-base overhangs. The results

Table 1. Influence of fluoxetine on phosphatidylserine exposure and DNA strand breaks in L3055 BL cells

Treatment†	Annexin V binding*		% TUNEL positive‡
	% positive	MFI	
Control	52.3 ± 1.8	3.9 ± 0.2	17.8 ± 3.7
Anti-IgM	94.5 ± 1.0	71.1 ± 12.1	51.7 ± 14.5
Fluoxetine	81.1 ± 3.9	26.1 ± 8.4	35.7 ± 7.6

*Samples analyzed by FACS to generate percent positive cells within the Annexin V$^+$/PI$^-$ "apoptotic" gate together with mean fluorescent intensity (MFI) of stain. Results are means ± SEMs of 3 separate experiments.

†L3055 cells were cultured at 10^6/mL for 17 hours in control medium, with anti-IgM (μ chain) at 10 μg/mL or fluoxetine at 20 μM.

‡Samples analyzed by FACS to generate percent nonsubdiploid cells (as assessed by PI stain) positive by TUNEL. Results are means ± SEs of 3 separate experiments.

showed a discernible (although not dramatic) increase in the number of L3055 cells with such breaks following their treatment with either anti-IgM or fluoxetine (Table 1).

Importantly, normal peripheral blood mononuclear cells (PBMCs) remained viable on exposure to SSRIs. The viability of cells exposed for 24 hours to 5 μM fluoxetine and to 10 μM fluoxetine was recorded as 97.3 ± 0.88% and 97.3 ± 0.33%, respectively compared with 98.0 ± 0.58% in control cultures. Even with 20 μM fluoxetine, viability remained at 83.7 ± 1.20%. A near identical outcome was noted with normal resting B cells isolated from tonsils, where viabilities after 24 hours of culture with control medium or fluoxetine at 5, 10, or 20 μM were 97.4 ± 0.53%, 97.0 ± 0.41%, 96.5 ± 0.88%, and 85.9 ± 1.07% respectively. To assess the possibility that SSRIs might selectively target B cells when actively cycling, tonsilar B cells were exposed overnight to fluoxetine following 2 days of stimulation either with SAC (alone or combined with soluble CD40L) or with phorbol myristate acetate (PMA; alone or in combination with ionomycin). As can be seen from Figure 3A, little inhibition of DNA synthesis occurred in any of the actively cycling populations even with fluoxetine present at 20 μM. Similarly, the clear inhibitory effect of fluoxetine on DNA synthesis in biopsy-like BL lines such as L3055 was not evident when assessed on 5 non-BL lines with either no, or only minor, reductions in the level of ^{3}[H]-thymidine incorporation observed in Nalm-6 ("pre-B"), RPMI 8226 ("plasmacytoid"), or the 3 T-cell lines: Jurkat, J10, and CEM (Figure 3B).

We wished to examine whether the observed resistance to SSRI-induced death among normal B cells related to a constitutive expression of Bcl-2[35] and how these levels compared with, and among, the biopsy-like BL lines and the non-BL lines studied here. Western blotting for Bcl-2 confirmed its low-level expression in wild-type L3055 cells and in those carrying empty vector; those transfected with *bcl-2* carried the expected high levels of the protein (Figure 3C). Two other group I BL lines, Elijah and Mutu I, carried undetectable levels of Bcl-2, whereas Namalwa carried detectable but still relatively low levels of the protein. Normal resting B cells from tonsils were confirmed as expressing high levels of Bcl-2 (Figure 3C). The 5 non-BL lines studied carried variable but readily detectable Bcl-2 (Figure 3D). When compared against the freshly isolated population, tonsilar B cells that had been activated for 2 days by PMA and ionomycin showed a relative down-regulation of Bcl-2 expression, although levels remained readily detectable. Independent measure of Bcl-2 content by FACS analysis performed as described previously[36] fully confirmed the findings made by Western blotting and additionally showed that PBMCs were at least as positive for Bcl-2 expression as purified resting tonsilar B cells (data not detailed). Although not available at

the time of this analysis, it has been well documented that Mutu III cells carry Bcl-2 protein at a level considerably higher than those of its Mutu I counterpart[35-37]; furthermore, a direct comparison of Bcl-2 levels in Mutu I, Mutu III, L3055 wild-type, and L3055/bcl-2 transfectants as assessed by Western blotting was comprehensively detailed by 2 of us in a recent study.[22] Likewise, we have previously demonstrated that BL2 cells carry low levels of Bcl-2 similar to L3055 cells.[21]

SSRIs directly stimulate signal transduction pathways and down-regulation of c-*myc* and *nm23* genes in BL cells

Apoptosis is an active process driven by diverse signal transduction pathways, among which an elevation in the level of intracellular free Ca^{2+} ($[Ca^{2+}]_i$) can be key.[29,38] SSRIs have variously been described as either direct inhibitors of Ca^{2+} channels or inducers of Ca^{2+} signaling in a diversity of cell types.[39-42] Here, we found that fluoxetine prompted a rapid rise in basal Ca^{2+} in BL cells with an EC_{50} close to that obtained for inhibition of DNA synthesis (Figure 4A). All 3 SSRIs promoted an increase in basal Ca^{2+} with a similar shape and kinetics (Figure 4B-D). Further study with fluoxetine indicated that (1) it acted on thapsigargin-sensitive endoplasmic reticulum Ca^{2+} stores and (2) triggered Ca^{2+} influx. Thus, (1) Figure 4E shows that, in low Ca^{2+} medium, fluoxetine addition failed to increase $[Ca^{2+}]_i$ following the depletion of Ca^{2+} from stores sensitive to thapsigargin[29] and (2) Figure 4F demonstrates that chelating extracellular Ca^{2+} with EGTA resulted in a substantial diminution of the rise in $[Ca^{2+}]_i$ provoked on fluoxetine addition.[29]

The concentrations of SSRIs required to promote elevations in intracellular-free Ca^{2+}, DNA synthesis cessation, and induction into apoptosis appear incompatible with their pharmacology at the serotonin transporter.[28,43] In an attempt to address whether their actions were targeted on SERT or not, we made use of the competitive binding that exists between fluoxetine and 5-HT at the
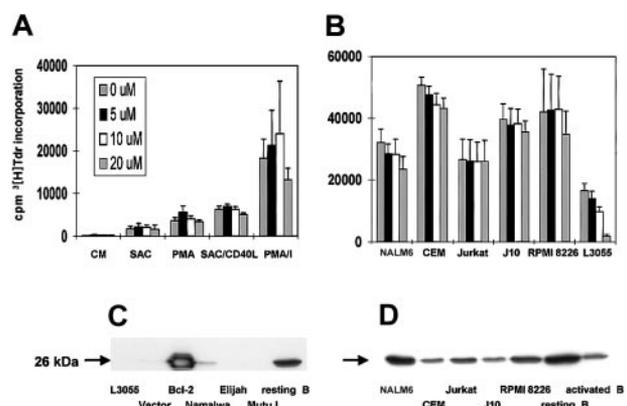

Figure 3. Fluoxetine actions on and Bcl-2 levels in normal B cells and non-BL cell lines. (A) Resting tonsilar B cells were cultured at 10^5 cells per 200 μL culture medium for 48 hours in flat-bottom microtiter wells with either no addition (CM), *Staphylococcus aureus* Cowan 1 (SAC, 1:10 000), phorbol 12-myristate 13-acetate (PMA, 5 ng/mL), SAC+sCD40L (1μg/mL), or PMA + ionomycin (PMA/I, 1 μg/mL), before addition of fluoxetine at 0 to 20 μM as indicated. Cells were then cultured for a further 24 hours, pulsed with ^{3}[H]-thymidine for the last 7 hours for the analysis of DNA synthesis. (B) Cells from lines indicated were cultured for 24 hours with fluoxetine as in panel A before assessment of DNA synthesis as described in Figure 1A-D. Data are means ± SEMs from 3 separate experiments. (C-D) Cell lysates were prepared from pelleted cells and equal amounts of protein (25 μg) resolved on 12.5% SDS-PAGE before blotting for Bcl-2, the protein migrating with an apparent molecular weight of 26 kDa as indicated. Panel C is a representative blot of protein from L3055 (wild type), L3055 vector controls, L3055/Bcl-2 transfectants, Namalwa, Elijah, Mutu I, and resting tonsilar B cells; panel D, from Nalm 6, CEM, Jurkat, J10, RPMI8226, resting tonsilar B cells, and B cells activated for 48 hours with PMA+ionomycin.

Figure 4. SSRIs trigger Ca²⁺ flux, tyrosine phosphorylation, and down-regulation of *c-myc* and *nm23* genes in group I BL cells. $[Ca^{2+}]_i$ measurements in L3055 cells treated with (A) 0.5 to 80 μM fluoxetine; (B) 20 μM fluoxetine; (C) 20 μM paroxetine; (D) 100 μM citalopram; (E) 100 nM thapsigargin (Thg) followed by 20 μM fluoxetine in Ca²⁺-low medium (addition of 20 μM fluoxetine alone in Ca²⁺-low medium indicated in insert); (F) 20 μM fluoxetine in the presence or absence of 9 mM EGTA; and (G) 20 μM fluoxetine in the presence or absence of 1 mM 5-HT. Each result either is representative or means ± SEMs of 3 experiments. (H) Western blotting analysis for protein phosphotyrosine in L3055 cells showing control (C) cultures and following treatment with 20 μM fluoxetine (Fl) or 10 μg/mL anti-μ chain antibody (Ig) for 60, 150, or 300 seconds. Blot is representative of 4 different experiments. (I) Real-time quantitative PCR analysis of indicated genes after 6 hours exposure of L3055 cells to 20 μM fluoxetine. Relative gene expressions normalized to L3055 control cultures (100%). Data are the means ± SEMs of 4 experiments each performed in triplicate.
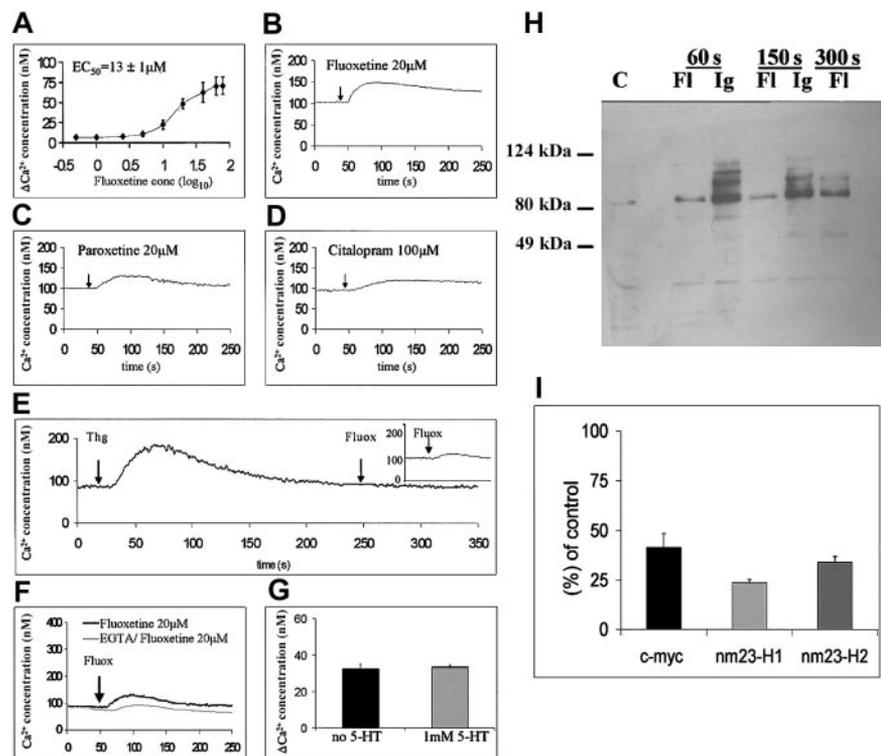
transporter.[44] While 5-HT, via SERT, can also drive apoptosis in BL cells[20] it does so without increasing basal levels of intracellular-free Ca²⁺ (n = 6; data not detailed). The inability of even a large (50 ×) excess of 5-HT to attenuate the fluoxetine-driven change in intracellular Ca²⁺ indicates that the actions of the latter—as detailed in this study—are most likely SERT-independent (Figure 4G).

In addition to elevating Ca²⁺, the SSRIs (as illustrated by fluoxetine) also prompted tyrosine phosphorylation on a number of protein substrates, of which 2 major ones—with apparent molecular weights of 85 and 105 kDa—were common to those targeted by antibody to surface IgM (albeit with different kinetics), a treatment which similarly liberates Ca²⁺ from intracellular stores and stimulates Ca²⁺ influx[29] (Figure 4H).

Despite its hallmark translocation to immunoglobulin loci, the BL-associated constitutive expression of *c-myc* remains dependent on the binding of the recognized *c-myc* transcription factor Nm23-H2 to a PuF site within the regulatory sequence of the translocated gene.[10] Using real-time RT-PCR, we found that a 6-hour exposure of biopsy-like BL cells to fluoxetine resulted in an approximate 60% reduction in the levels of both *nm23*-H2 and *c-myc* (Figure 4I). We also observed a rapid 75% decrease in the expression of *nm23*-H1 mRNA, the product of which has also been linked to *c-myc* expression.[11] In contrast, expression of the housekeeping gene cyclophilin A was not significantly altered, with levels remaining at 81.8% (SE = 8.3%) of control values following fluoxetine treatment ($P = .16$).

Discussion

Our findings reported herein demonstrate that the SSRI class of antidepressants are capable of driving programmed death among the constituent cells of Burkitt lymphoma, a highly aggressive tumor that remains problematic in areas where it is endemic and

that has increased dramatically worldwide because of an association with AIDS.[1-6,45] The present study was prompted by our recent finding that BL cells carry the serotonin transporter and are susceptible to programmed death resulting from the uptake of 5-HT; however, in itself, the monoamine is not a deliverable drug.[20] During those studies we noted that at concentrations only slightly higher than those required for blocking serotonin-promoted apoptosis, the SSRIs began to exhibit what appeared to be direct inhibitory effects on biopsy-like BL cells maintained in early passage.[20] This preliminary observation led us to explore possible proapoptotic activity of the SSRIs in their own right.

Each of the 3 structurally distinct SSRIs[43] investigated was found capable of driving cessation of DNA synthesis in group I BL cells remaining faithful to the original biopsy phenotype. Inhibition of S-phase entry correlated with a relative accumulation of cells in the G_0/G_1 phase of cell cycle and was accompanied by extensive cell death that displayed features of apoptosis: characteristic cell shrinkage with increased granularity; loss of viability with retained membrane integrity against propidium iodide; phosphatidylserine exposure; nuclear condensation and fragmentation; caspase activation; cleavage of PARP-1; DNA fragmentation; and decreased mitochondrial membrane potential. SSRI-induced BL cell death could be effectively reversed either by engaging the CD40 prosurvival pathway or ectopically expressing antiapoptotic *bcl*-2. Similarly, the refractoriness of late-passage Mutu III cells to the SSRI actions is consistent with the apoptotic pathway activated in the sensitive group I lines in that the turn on of EBV-latent genes as cells drift to the group III phenotype is accompanied by a general resistance to apoptosis-inducing stimuli.[18,19,27,36] Both peripheral blood mononuclear cells and purified resting tonsilar B cells were largely refractory to SSRI-induced cell death that, again, may partly relate to a constitutive expression of the requisite survival genes, although the role of other factors also needs to be considered.[35] The effects of the SSRIs against BL cells did not simply

reflect the fact that they were cycling: 5 randomly chosen non-BL lymphoid lines were largely immune to the actions of the SSRIs as were tonsilar B cells that had been stimulated into cycle by polyclonal mitogens. Germinal center B cells, the phenotypic normal counterparts to BL, enter apoptosis spontaneously ex vivo,[14-17] and the preliminary indications are that SSRIs do not perceptibly alter the kinetics of this intrinsic programmed death (A.S., M.J.H., and J.G., unpublished observations, June 2001). Encouragingly, therefore, it appears that with respect to the apoptotic pathway of death the SSRIs preferentially target the proliferating BL cell. Whether other B-cell malignancies in which the constitutive cells display a propensity for apoptosis induction (for example, chronic lymphocytic leukemia[26]) might also be sensitive to the actions of SSRIs is currently under investigation.

All 3 SSRIs were seen to provoke a rise in the basal level of intracellular-free Ca^{2+} in biopsy-like BL cells. We examined this possibility, in part as it is known that a rise in $[Ca^{2+}]_I$ can be key to initiating the apoptotic cascade in BL cells—for example in response to BCR cross-linking[29]—but also from reports on other cell types indicating that SSRIs can directly affect Ca^{2+} flux, either negatively or positively. Thus, fluoxetine has been shown to block voltage-gated calcium channels in rat hippocampal pyramidal cells[39] and in PC12 cells[41] (derived from rat adrenal medulla chromaffin cells) with an IC_{50} of 6.8 and 13.4 μM, respectively, while stimulating a Ca^{2+} flux in Madin-Darby canine kidney cells[42] and bladder female transitional carcinoma (BFTC)[40] cells with an EC_{50} of 40 and 30 μM, respectively. While the concentration of fluoxetine required to elicit a Ca^{2+} response in BFTC cells was more than twice that noted in the present study for BL cells, the characteristics were remarkably similar—notably the provoking of Ca^{2+} release from thapsigargin-sensitive intracellular stores and the induction of Ca^{2+} influx from the extracellular medium.[40] This pattern also bears similarities to the elevation in Ca^{2+} prompted in BL cells on ligating BCR where a direct causal relationship has been established between this change and subsequent apoptosis.[29] It was of interest that both exposure to SSRIs and ligation of BCR stimulated in BL cells tyrosine phosphorylation with at least 2 of the protein substrates common to the 2 triggers, suggesting some parallels in the signaling pathways engaged.

The concentrations of SSRIs required to promote change in biopsy-like BL cells appear incompatible with their pharmacology at the serotonin transporter; indeed, the inability of even a 50-fold excess of 5-HT to compete out the fluoxetine-induced Ca^{2+} rise indicates that their actions reported herein are possibly SERT-independent.[28,43,44] Nonserotonergic effects of fluoxetine have been reported,[46-48] and it will be of interest to determine the molecular target(s) for the direct actions of the SSRI on BL cells.

BL is characterized by translocations of one c-myc allele to one of the immunoglobulin loci, and the extraordinarily high growth rate that characterizes these tumors reflects the proproliferative actions of the translocated gene.[7] However, despite translocation to immunoglobulin loci, the BL-associated constitutive expression of c-myc remains dependent on the binding of the recognized c-myc transcription factor Nm23-H2 to a PuF site within the regulatory sequence of the translocated gene.[10] Here we found, using real-time RT-PCR, that a 6-hour exposure to fluoxetine resulted in reductions in the levels of both nm23-H2 and c-myc and also of nm23-H1. A

recent report has identified that Nm23-H1 may also be linked to c-myc expression.[11] Thus the SSRIs appear to influence the very genes that underpin the uncontrolled cell division normally associated with BL. Furthermore, high expression of Nm23-H1 has been correlated with poor responses to treatment in high-grade lymphomas other than BL.[12] These observations may therefore have implications for the clinical exploitation of SSRIs in the broader context of B-cell lymphoma. Although a constitutively high bcl-2 expression could potentially compromise such hope, the possibility of combining the delivery of SSRIs with, for example, targeted antisense strategies, could keep this wider possibility open.[49]

The concentrations of SSRIs shown to be active against BL cells (eg, fluoxetine, EC_{50} = 9.3 ± 2.3 μM for cessation of DNA synthesis) are higher than those seemingly achieved with the current therapeutic use of these drugs for depression and anxiety-related disorders.[43] After 30 days of dosing at 40 mg/d, plasma concentrations of fluoxetine, for example, reach no more than 1 μM.[43] However, SSRIs are highly lipophilic and may accumulate in tissues: for example, in one study an estimate of 20:1 was given for the relative partition of fluoxetine between brain and blood.[50] Interestingly, while Bolo et al[51] reported a somewhat lower brain-to-plasma ratio of 10:1, the average concentration of fluoxetine found in brain for 12 subjects taking between 10 and 40 mg per day was 13 μM, a figure slightly above the EC_{50} obtained for the ability of the drug to inhibit DNA synthesis in BL cells. Yet another study[52] confirmed the high accumulation of fluoxetine into tissue spaces with an apparent distribution volume of 12 to 43 in brain relative to plasma. Moreover, SSRIs can be administered at levels much higher than those currently prescribed without major side effects. From an extensive survey of the literature, Barbey and Roose[53] concluded that taking amounts up to 30 times the common daily dose is associated with either minor or no undesirable symptoms; even ingestions of greater amounts typically resulted in—at worst—drowsiness, tremor, nausea, and vomiting. Only at higher than 75 times the normal dose did more serious adverse events occur. Indeed, one of the perceived benefits of SSRIs over, for example, the tricyclic antidepressants, is that fatalities through overdosing are extremely rare and usually result from combination with other drugs.[43,53]

While the above pharmacokinetic considerations seem encouraging in relation to our in vitro data, it is clear that more work is required before the SSRIs can be considered as deliverable therapeutics for patients with Burkitt lymphoma; for example, issues such as whether autonomously produced CD40L could potentially counter the proapoptotic actions of SSRIs in situ need to be addressed.[54] The availability of well-characterized animal models of BL will allow the necessary next stages of such a goal to be investigated in detail.[55,56]

Acknowledgments

References

1. Berard C, O'Conor GT, Thomas LB, Torloni H. Histopathological definition of Burkitt's lymphoma. Bull WHO. 1969;40:601-607.

2. O'Conor GT. Malignant lymphoma in African children: II. pathological entity. Cancer. 1961;14:270-283.

3. Magrath IT. Management of high-grade lymphomas. Oncology (Huntingt). 1998;12:40-8.

4. Coté TR, Biggar RJ, Rosenberg PS, et al. Non-Hodgkin's lymphoma among people with AIDS: incidence, presentation and public health burden. AIDS/Cancer Study Group. Int J Cancer. 1997; 73:645-650.

5. Herndier BG, Kaplan LD, McGrath MS. Pathogenesis of AIDS lymphomas. AIDS. 1994;8:1025-1049.

6. Oksenhendler E, Gerard L, Dubreuil ML, et al. Intensive chemotherapy (LNHIV-91 regimen) and G-CSF for HIV associated non-Hodgkin's lymphoma. Leuk Lymphoma. 2000;39:87-95.

7. Klein G, Klein E. Myc/Ig juxtaposition by chromosomal translocations: some new insights, puzzles, and paradoxes. Immunol Today. 1985;6:208-215.

8. Heikkila R, Scwab G, Wickstrom E, et al. A c-myc antisense oligodeoxynucleotide inhibits entry into S-phase but not progress from G0 to G1. Nature. 1987;328:445-449.

9. Evan G, Littlewood T. The role of c-myc in cell growth. Curr Opin Genet Dev. 1993;3:44-47.

10. Ji L, Arcinas M, Boxer LM. The transcription factor, Nm23H2, binds to and activates the translocated c-myc allele in Burkitt's lymphoma. J Biol Chem. 1995;270:13392-13398.

11. Godfried MB, Veenstra M, v Sluis P, et al. The N-myc and c-myc downstream pathways include the chromosome 17q genes nm23-H1 and nm23-H2. Oncogene. 2002;21:2097-2101.

12. Niitsu N, Okabe-Kado J, Okamoto M, et al. Serum nm23-H1 protein as a prognostic factor in aggressive non-Hodgkin lymphoma. Blood. 2001;97:1202-1210.

13. Epstein MA, Herdson PB. Cellular degeneration associated with characteristic nuclear fine structure changes in the cells from two cases of Burkitt's malignant lymphoma syndrome. Brit J Cancer. 1963;17:56-58.

14. Rooney CM, Gregory CD, Rowe M, et al. Endemic Burkitt's lymphoma: phenotypic analysis of tumour biopsy cells and of derived tumor cell lines. J Natl Cancer Inst. 1986;77:681-687.

15. Gregory CD, Edwards CF, Milner A, et al. Isolation of a normal B cell subset with a Burkitt-like phenotype and transformation in vitro with Epstein-Barr virus. Int J Cancer. 1988;42:213-220.

16. MacLennan ICM. Germinal centers. Annu Rev Immunol. 1994;12:117-139.

17. Holder MJ, Wang H, Milner AE, et al. Suppression of apoptosis in normal and neoplastic human B lymphocytes by CD40 ligand is independent of Bcl-2 induction. Eur J Immunol. 1993;9:2368-2371.

18. Gregory CD, Rowe M, Rickinson AB. Different Epstein-Barr virus B cell interactions in phenotypically distinct clones of a Burkitt's lymphoma cell line. J Gen Virol. 1990;71:1481-1495.

19. Rowe M, Rowe DT, Gregory CD, et al. Differences in B cell growth phenotype reflect novel patterns of Epstein-Barr virus latent gene expression in Burkitt's lymphoma cells. EMBO J. 1987;6:2743-2751.

20. Serafeim A, Grafton G, Chamba A, et al. 5-Hydroxytryptamine drives apoptosis in biopsylike Burkitt lymphoma cells: reversal by selective serotonin reuptake inhibitors. Blood. 2002;99:2545-2553.

21. Baker MP, Eliopoulos E, Young LS, Armitage RJ, Gregory CD, Gordon J. Prolonged phenotypic, functional, and molecular change in group I Burkitt lymphoma cells on short-term exposure to CD40 ligand. Blood. 1998;92:2830-2843.

22. Gordon J, Challa A, Levens JM, et al. CD40 Ligand, Bcl-2, and Bcl-x$_L$ spare Group I Burkitt lymphoma cells from CD77-directed killing via Verotoxin-1 B chain but fail to protect against the holotoxin. Cell Death Diff. 2000;7:785-794.

23. McCloskey N, Poun JD, Holder J, et al. The extrafollicular-to-follicular transition of human B lymphocytes: induction of functional globotriaosylceramide (CD77) on high threshold occupancy of CD40. Eur J Immunol. 1999;29:3236-3244.

24. MacDonald I, Wang H, Grand R, et al. Transforming growth factor-β1 cooperates with anti-immunoglobulin for the induction of apoptosis in group I (biopsy-like) Burkitt lymphoma cell lines. Blood. 1996;87:1147-1154.

25. Milner AE, Palmer DH, Hodgkin EA, et al. Induction of apoptosis by chemotherapeutic drugs: the role of FADD in activation of caspase-8 and synergy with death receptor ligands in ovarian carcinoma cells. Cell Death Differ. 2002;9:287-300.

26. Baker PK, Pettitt AR, Slupsky JR, et al. Response of hairy cells to IFN-α involves induction of apoptosis through autocrine TNF-α and protection by adhesion. Blood. 2002;100:647-653.

27. Gregory CD, Dive C, Henderson S, et al. Activation of Epstein-Barr virus latent genes protects human B cells from death by apoptosis. Nature. 1991;349:612-614.

28. Ramamoorthy S, Bauman AL, Moore KR, et al. Antidepressant- and cocaine-sensitive human serotonin transporter: molecular cloning, expression, and chromosomal localization. Proc Natl Acad Sci U S A. 1993;90:2542-2546.

29. Grafton G, Goodall M, Gregory CD, Gordon J. Mechanisms of antigen receptor-dependent apoptosis in human B lymphoma cell lines probed with a panel of 27 monoclonal antibodies. Cell Immunol. 1997;182:45-56.

30. Dive C, Gregory CD, Phipps DJ, Evans DL, Milner AE, Wyllie AH. Analysis and discrimination of necrosis and apoptosis (programmed cell death) by multiparameter flow cytometry. Biochimica Biophysica Acta. 1992;1133:275-285.

31. Dillon SR, Constantinescu A, Schlissel MS. Annexin V binds to positively selected B cells. J Immunol. 2001;166:58-71.

32. Hammill AK, Uhr JW, Scheuermann RH. Annexin V staining due to loss of membrane asymmetry can be reversible and precede commitment to apoptotic death. Exp Cell Res. 1999;251:16-21.

33. Nakamura M, Yagi H, Kayaba S, et al. Death of germinal center B cells without DNA fragmentation. Eur J Immunol. 1996;26:1211-1216.

34. Luciano F, Ricci JE, Herrant M, et al. T and B leukemic cell lines exhibit different requirements for cell death: correlation between caspase activation, DFF40/DFF45 expression, DNA fragmentation and apoptosis in T cell lines but not in Burkitt's lymphoma. Leukemia. 2002;16:700-707.

35. Liu YJ, Mason DY, Johnson GD, et al. Germinal center cells express bcl-2 protein after activation by signals which prevent their entry to apoptosis. Eur J Immunol. 1991;21:1905-1910.

36. Henderson S, Rowe M, Gregory C, et al. Induction of bcl-2 expression by Epstein-Barr virus latent membrane protein 1 protects infected B cells from programmed cell death. Cell. 1991;65:1107-1115.

37. Milner AE, Johnson GD, Gregory CD. Prevention of programmed cell death in Burkitt lymphoma cell lines by bcl-2-dependent and bcl-2-independent mechanisms. Int J Cancer. 1992;52:636-644.

38. Krebs J. The role of calcium in apoptosis. Biometals. 1998;11:375-382.

39. Deak F, Lasztoczi B, Pacher P, Petheo GL, Kecskemeti V, Spat A. Inhibition of voltage-gated calcium channels by fluoxetine in rat hippocampal pyramidal cells. Neuropharmacology. 2000;38:1029-1036.

40. Tang KY, Lu T, Chang CH, et al. Effect of fluoxetine on intracellular Ca2+ levels in bladder female transitional carcinoma (BFTC) cells. Pharmacol Res. 2001;43:503-508.

41. Hahn SJ, Choi JS, Rhie DJ, Oh CS, Jo YH, Kim MS. Inhibition by fluoxetine of voltage-activated ion channels in rat PC12 cells. Eur J Pharmacol. 1999;367:113-118.

42. Tang KY, Cheng JS, Lee KC, et al. Fluoxetine-induced Ca2+ signals in Madin-Darby canine kidney cells. Naunyn Schmiedebergs Arch Pharmacol. 2001;363:16-20.

43. Preskorn SH. Clinical Pharmacology of Selective Serotonin Reuptake Inhibitors. Caddo, OK: Professional Communications; 1996.

44. Marcusson JO, Bergström M, Eriksson K, Ross SB. Characterization of [3H]paroxetine binding in rat brain. J Neurochem. 1988;50:1783-1790.

45. Beral V, Peterman T, Berkelman R, Jaffe H. AIDS-associated non-Hodgkin lymphoma. Lancet. 1991;337:805-809.

46. Ranganathan R, Sawin ER, Trent C, Horvitz HR. Mutations in the *Caenorhabditis elegans* serotonin reuptake transporter MOD-5 reveal serotonin-dependent and –independent activities of fluoxetine. J Neurosci. 2001;21:5871-5884.

47. Choy RK, Thomas JH. Fluoxetine-resistant mutants in C. elegans define a novel family of transmembrane proteins. Mol Cell 1999;4:143-152.

48. Garcia-Colunga J, Awad JN, Miledi R. Blockage of muscle and neuronal nicotinic acetylcholine receptors by fluoxetine (Prozac). Proc Natl Acad Sci U S A. 1997;94:2041-2044.

49. Cotter FE, Waters J, Cunningham D. Human Bcl-2 antisense therapy for lymphomas. Biochim Biophys Acta. 1999;1489:97-106.

50. Karson CN, Newton JE, Livingston R, et al. Human brain fluoxetine concentrations. J Neuropsychiatry Clin Neurosci. 1993;5:322-329.

51. Bolo NR, Hode Y, Nedelec JF, Laine E, Wagner G, Macher JP. Brain pharmacokinetics and tissue distribution in vivo of fluvoxamine and fluoxetine by fluorine magnetic resonance spectroscopy. Neuropsychopharmacology. 2000;23:428-438.

52. Altamura AC, Moro AR, Percudani M. Clinical pharmacokinetics of fluoxetine. Clin Pharmacokinet. 1994;26:201-214.

53. Barbey JT, Roose SP. SSRI safety in overdose. J Clin Psychiatry. 1998;59(suppl 15):42-48.

54. Challa A, Eliopoulos AG, Holder M, et al. Population depletion activates autonomous CD154-dependent survival in biopsy-like Burkitt's lymphoma cells. Blood. 2002;99:3411-3418.

55. Murphy WJ, Taub DD, Longo DL. The huPBL-SCID mouse as a means to examine human immune function in vivo. Semin Immunol. 1996;8:233-241.

56. Kovalchuk AL, Qi CF, Torrey TA, et al. Burkitt lymphoma in the mouse. J Exp Med. 2000;192:1183-1190.